A PROOF-OF-PRINCIPLE EXPERIMENT FOR A STRUCTURE-LOADED CO$_2$ LASER-DRIVEN ELECTRON ACCELERATOR IN VACUUM

Yuan-Yao Lin, Yen-Chieh Huang, and An-Chung Chiang, National Tsinghua University, Taiwan

Abstract

The experimental realization of structure-loaded laser-driven particle acceleration in vacuum is crucial for developing next-generation high-gradient particle accelerators. We report the status of a proof-of-principle experiment for structure-loaded laser-driven electron acceleration. A single-stage CO$_2$ laser-driven accelerator is fabricated and optically tested for providing 150 keV energy gain to a 70 MeV electron beam over a 10-cm stage length. A resonant-type lens-array accelerator structure consisting of 16 properly phased acceleration stages is also fabricated and optically tested for realizing multi-stage laser-driven electron acceleration in vacuum. In this paper, we present the acceleration scheme, structure fabrication, challenges, goals, and status of the experiment.

INTRODUCTION

Laser-driven particle acceleration, if realized, has the advantage of providing high acceleration gradients and producing ultra-short electron bunches. These unique features will benefit to the applications in radiation and high energy physics. For schemes adopting linear acceleration, numerous experimental evidences have been generated from plasma-based laser-driven accelerators. To date, there is still no evidence of laser-driven particle acceleration in a hard-structure linear accelerator (linac) in vacuum. One major difficulty is that the accelerator dimension is too small to operate at the laser wavelength [1]. To conduct a proof-of-principle experiment at the Accelerator Test Facility (ATF), Brookhaven National Laboratory (BNL), we discuss in this paper the design and fabrication of large-size single-stage and multistage CO$_2$ laser-driven linac's. The primary design consideration is to have a large energy gain, a macroscopic size, and a structure that is flexible enough for investigating accelerator physics. Although a high acceleration gradient is not considered for a proof-of-principle experiment, the acceleration gradient can be further improved as soon as the experimental evidence for vacuum linear acceleration is obtained.

SINGLE-STAGE WAVEFRONT-SPLITTING ACCELERATOR

A cross-beam laser-driven accelerator utilizes two phase reversed, crossed, TEM$_{00}$ Gaussian laser beams [2-3] to form the particle acceleration field. A single-stage wavefront-splitting laser-driven accelerator is a variant of the cross-beam accelerator. Figure 1 depicts the schematic of a wavefront-splitting accelerator structure [4]. The structure consists of a corner reflector for dividing the laser wavefront and synthesizing the acceleration field and a downstream 45° reflector for bringing in and terminating the laser fields. The edge of the corner reflector forms an angle θ with respect to the x direction. Both the corner reflector and the 45° reflector have an aperture for transmitting electrons. This simple design does not employ any laser mode for particle acceleration, but obtains the particle acceleration field by combining two properly phased TM polarized waves from the corner reflector. These two plane waves can be split from an enlarged TEM$_{00}$ laser beam, as shown by the laser coupling configuration in Fig. 1. The corner reflector divides the single-wavefront laser beam coming from the 45° coupling mirror into two halves and recombines the two waves inside the accelerator structure. The relative phase of the two half plane waves can be adjusted, for example, by varying the longitudinal position of one arm of the corner reflector. The phase tuning resolution can be 0.6 mrad/nm by using a PZT controlled M1 or M2 capable of moving nanometer steps over a ~10-nm distance. When the optical paths between the two plane waves differ by a half wavelength, the transverse fields of the two plane waves cancel each other and the longitudinal fields add to provide the acceleration field.
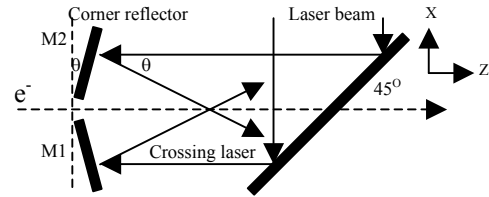

Figure 1: The configuration of the single-stage accelerator structure. The particle acceleration field is derived from two properly phased waves reflected from a corner reflector. The 45° reflector is used for coupling the input laser beam and terminating the laser fields.

Assume that a π phase shift is pre-arranged for two equal-amplitude plane waves. In the plane-wave approximation, the laser field in the z direction can be written as

$$E_z = 2E_0 \cos(\omega t - k\cos\theta \cdot z + \phi) \cdot \cos(k\sin\theta \cdot x) \times \sin\theta, \quad (1)$$

where E_0 is the electrical field amplitude associated with each plane wave, ϕ is an arbitrary initial phase, and ω is the angular frequency, k is the wave number of the laser field, and θ is the crossing angle defined in Fig. 1. In the electron rest frame, the acceleration field seen by an on-axis electron is given by

$$E_{z,e} = 2E_0 \sin\theta \cos[kz(1/\gamma^2 + \theta^2)/2 + \phi], \quad (2)$$

where $v_e = c(1-1/\gamma^2)^{1/2}$ is the electron velocity with γ being the Lorentz factor and c the vacuum wave velocity. In the expression, a small crossing angle $\theta \ll 1$ and a large electron energy $\gamma \gg 1$ is assumed. By calculating $\partial U/\partial \theta = 0$, it is possible to obtain the laser crossing angle θ at which the electron energy gain, $U = \int E_{z,e} dz$, reaches maximum. As a result, the maximum electron energy gain can be obtained

$$U_{max} = \frac{2\gamma}{\pi} \lambda E_0 = \frac{2\gamma}{\pi} \lambda \sqrt{2\eta_0 I}, \qquad (3)$$

at $\theta = 1/\gamma$, where η_0 is the vacuum wave impedance, λ is the laser wavelength, and I is the laser intensity.

Given a material, a laser wavelength, and a laser pulse width, the maximum laser damage intensity I to an accelerator structure is fixed. Therefore, the maximum electron energy gain is predominantly dependent on the electron energy γ and the laser wavelength λ. A large γ and a longer λ help to reduce the phase slippage and permit the use of a larger structure size. In addition, for structure-based laser driven linear acceleration, one has to open electron transit holes comparable, or larger than the driving wavelength in the accelerator structure [5]. In the corner reflector design, the leakage field through the electron transit hole reduces the acceleration field, whereas the leakage field through the hole in the 45° reflector partially removes the electron energy gained in the accelerator structure. To estimate the energy gain reduction, we employ two-dimensional synthesized plane waves to model the electric fields at the electron transit hole.
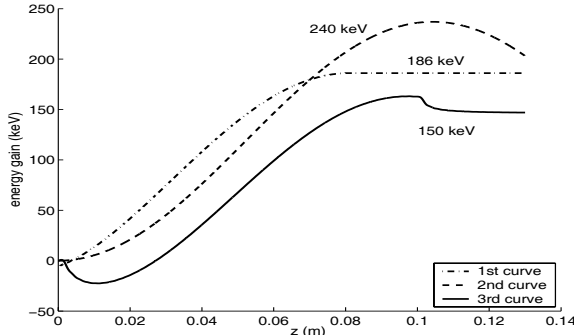

Figure 2. 1st curve: Electron energy gain calculated from Eq. (2). 2nd curve: energy gain including the effect of the finite reflector size and termination of the laser field. 3rd curve: energy gain with the consideration of the 200-μm electron transit holes.

Figure 2 shows the electron energy gain, integrated over the accelerator length with $\lambda = 10.6$ μm, $\theta = 1/\gamma = 7$ mrad, and $E_0 = 0.25$ GV/m which is the damage field of copper that we measured using ATF's 200-ps CO_2 laser. The 1st curve was calculated from Eq. (2), yielding 240 keV maximum energy gain within a 10-cm acceleration distance. The 2nd curve includes the effect of the finite size of the corner reflector and termination of the laser field at the 45° reflector, yielding 186 keV energy gain.

The 3rd curve further takes into the consideration of the leakage fields through the 200-μm electron transit hole, yielding 150 keV energy gain. As can be seen from Fig. 2, the gain reduction is about 20% with an electron transit aperture about 20 times the driving wavelength. Therefore, with the design parameters, one can expect a maximum energy gain of 150 keV from such a simple, single-stage accelerator structure at the 0.25 GV/m material damage field. This amount of energy gain should be able to be measured conclusively by using the energy spectrometer with 10^{-4} resolution at ATF, BNL. In addition, the spatial period of the interference field for the CO_2 wavelength is more than 750 μm, which is large enough to accommodate the high-brightness electron beam at ATF, BNL.

MULTISTAGE LENS-ARRAY LINAC

To further understand beam loading, phase synchronization, and mode coupling of an accelerator, a resonant accelerator structure consisting of multiple accelerator stages is required. Figure 3 shows the design for a 16-stage lens-arrayed structure. M. O. Scully has proposed a similar structure with on-axis drift tubes for phase control [6]. The phase control of our design is achieved by varying the temperature of each lens. There is a 100-μm radius electron transit hole on each lens. This resonant structure supports a TEM_{01} laser mode, which is the desired particle acceleration field.
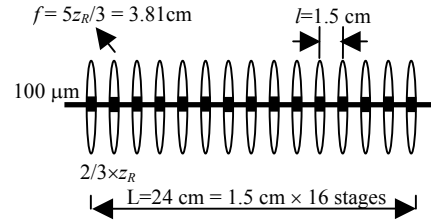

Figure 3: The multistage laser-driven linac.

E.J. Bochove *et al.* have analyzed the particle acceleration field in a TEM_{01} laser mode [7]. With a known transverse field in the TEM_{01} laser mode, the laser field along the z direction can be calculated from the charge-free and material-free Gauss law $\nabla \cdot \boldsymbol{E} = 0$. In the paraxial limit, the z-component electric field phasor is approximately given by

$$\widetilde{E}_z \approx \frac{-j}{k}\left(\frac{\partial \widetilde{E}_T}{\partial x} + \frac{\partial \widetilde{E}_T}{\partial y}\right), \qquad (4)$$

where $\widetilde{E}_T$ is the phasor of the transverse laser field. Based on Eq. (4), we again apply the synthesized-plane-wave method to numerically calculate the acceleration field and the electron energy gain in this multistage accelerator structure. In the computer simulation, the amplitude transmittance of the lens is given by

$$t = \begin{cases} \exp[-jk(d_0 - x^2/2R)(n-1) - jkd_0] \\ \exp(-jkd_0) \end{cases} \text{ for } \begin{cases} |x| > h/2 \\ |x| < h/2 \end{cases}, \quad (5)$$

where d_0= 1 mm is the thickness of the lens at $x = 0$, n is the refractive index of the lens, $R = f(n-1)$ is the radius of curvature on the convex lens surface, and h is the electron transit hole radius. Since we would like to have a large electron transit hole for transmitting electrons, we arbitrary chose 100 μm as the hole radius. To reduce the energy loss due to the leakage field from the electron transit holes, we design a laser waist radius about three times the electron transit hole radius. As a result, we started with $f = 3.81$ cm for our simulation, which gives l = 1.5 cm from the resonance condition. In the simulation, we assume that the lens can provide an arbitrary phase shift to the laser field so that the laser phase in each stage is optimized for maximum acceleration. This can be done by varying the temperature T of the dielectric lens by using a thermal-electric temperature controller. For ZnSe, the temperature dependence of the refractive index is $dn/dT = 5.7 \times 10^{-5}/°C$. For a 1-mm thick ZnSe, the CO_2 laser phase varies 180° for a 93°C temperature change.
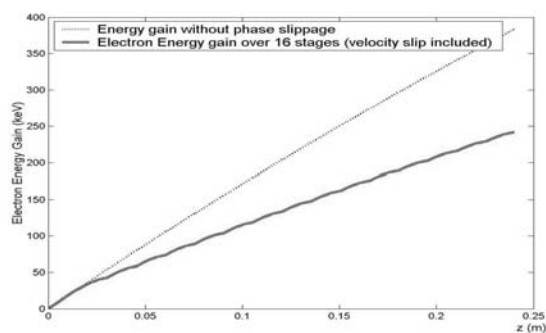

Figure 4: The electron energy gain versus distance over the 16-stage accelerator structure with and without electron velocity slippage. For 70-MeV electron injection energy, the total electron energy gain is about 240 keV.

The performance of the TEM_{01} lens-array waveguide was characterized by the calculating the overlapping integral of the resulting guiding field in the lens-array structure and a TEM_{01} laser field. Our calculation showed that this structure confines more than 80% of the energy in TEM_{01} mode over the 16 stages accelerator structure. Figure 4 is the accumulated electron energy gain over the 16 accelerator stages. The upper line is the energy gain versus distance without considering the electron velocity slippage, and the lower line is that with the velocity slippage at 70-MeV injection energy. At finite injection energy, the electron energy gain is influenced by the leakage field through the electron transit hole, because the widened laser angular spectrum contains many high-phase-velocity field components that slip ahead the electron and decelerate electrons. With our design parameters, the total energy gain for this multistage accelerator is about 240 keV at the laser damage threshold of 0.132 GV/m on ZnSe [8].

We have fabricated the 16-stage lens array accelerator and conducted some preliminary optical tests. The phase tuning was conducted by a 5 mW HeNe laser as a phase monitor. A 180° phase shift was observed over a 2 °C temperature change in a ZnSe lens of thickness $d = 0.98$mm. For the 16-stage structure, we developed an etlon-interferometry based optical alignment procedure that was experimentally demonstrated to achieve 20-μm alignment accuracy.

In Summary, we have reported the status of a proof-of-principle experiment for structure-loaded laser-driven electron acceleration. First, a wavefront-splitting, single-stage CO_2 laser-driven accelerator is being fabricated to provide 150 keV energy gain to a 70 MeV electron beam over a 10-cm stage length. Second, a resonant-type lens-array accelerator structure consisting of 16 properly phased acceleration stages was fabricated and optically tested for realizing multi-stage laser-driven electron acceleration in vacuum. The lens-array structure is estimated to provide 240 keV energy gain to a 70 MeV electron beam over a 24-cm total acceleration distance.

ACCKNOWLEDGEMENT

REFERENCES

[1] Y.C. Huang, D. Zheng, W.M. Tulloch, and R.L. Byer, "Proposed Structure for a Crossed-laser Beam, GeV per meter gradient, Vacuum Electron Linear Accelerator," *Appl. Phys. Lett.* **68** (1996) 753

[2] R.H. Pantell, Piestrup, "Free-electron momentum modulation by means of limited interaction length with light", *Appl. Phys. Lett.* **32** (1978) 781.

[3] Y.C. Huang and R.L. Byer, *Nucl. Inst. Meth.* A **393**, (1997) II-37.

[4] Y.C. Huang, "Particle Acceleration Field derived from a Wavefront-divided Gaussian Beam," *Opt. Comm.* **157** (1998) 145-149.

[5] Y.C. Huang and R.L. Byer, "Acceleration-field Calculation for a Structure-based Laser-driven Linear Accelerator", Rev. Sci. Instrum., **69,** No. 7 (1998) 2629.

[6] M.O. Scully, "A Simple Laser Linac," *Appl. Phys*. B **51**, (1990) 238-241

[7] E.J. Bochove, G.T. Moore, and M.O. Scully, "Acceleration of Particles by an Asymmetric Hermite-Gaussian Laser Beam," *Physical Review A*, **46**, No. 10, (1992) 6640.

[8] A.C. Chiang, Y.Y. Lin, Y.C. Huang, M. Babzien, "Laser-induced damage threshold at chemical vapor deposition grown diamond surfaces for 200-ps CO_2 laser pulses", *Opt. Lett.* **27** (2002) 164.

[9] R. Bonifacio, L. De. Salvo, P. Pierini, N. Piovella, and C. Pellegrini, "Spectrum, temporal structure and fluctuations in a high-gain free-electron laser starting from noise," *Phy. Rev. Lett.* **73** (1994) 70.